Proceedings World Geothermal Congress 2000
Kyushu - Tohoku, Japan, May 28 - June 10, 2000

NUMERICAL MODELING OF THE MIRAVALLES GEOTHERMAL FIELD, COSTA RICA

Minh Pham[1], Subir Sanyal[1], Eduardo Granados[1], Alfredo Mainieri[2] and Carlos Gonzáles[2]
[1]GeothermEx, Inc., 5221 Central Avenue, Suite 201, Richmond, California 94804 (USA)
[2]Instituto Costarricense de Electricidad, Sabana Norte, Piso 8, Dept. Estudios Geotérmicos, San José, Costa Rica

Key Words: initial-state, forecasting, reservoir behavior, data matching, Miravalles

ABSTRACT

Miravalles geothermal field has about 150 MW installed plant capacity being supplied by 24 active wells; more than 45 production/injection wells have been drilled to date in this field. A three-dimensional, finite-differences, numerical simulation model of the field was developed based on a conceptual model derived from extensive geological, geophysical and geochemical exploration data and results of drilling and testing of wells. The model was then calibrated by matching the initial state by trial and error. The model covers an area of 108 km^2 and consists of 6 layers of non-uniform thickness, with about 2,000 gridblocks in total. To further calibrate the model, detailed production and injection data from the wells were input into the model and the observed reservoir pressure histories were matched by trial and error. Production enthalpy data were available but were not particularly useful for matching, since the data showed little change during the three-year history. Historical geochemical data trends obtained from the production wells were used to constrain the model.

The calibrated numerical model, complemented by wellbore simulation, was then used to forecast reservoir behavior and individual well performance under a wide variety of production and injection schemes. These schemes included several expansion scenarios and the results were used in planning the production well drilling schedule for the purpose of maintaining the steam supply. Additionally, from these forecasts, an optimum production and injection strategy was developed; specifically, more infield injection was found to be necessary to ensure longevity of steam production.

1. INITIAL-STATE MODELING

1.1 Introduction

The Miravalles geothermal field is located in the Guanacaste Province of Costa Rica. Two single-flash units of 55 MW each are installed in this field and have been in operation since March 1994 and October 1998, respectively. In addition, a small backpressure unit of 5 MW capacity was put on line in 1995. It appears that the limit of possible expansion of the production area has effectively been reached in the northern, western and southern sectors of the field. At present, studies are being undertaken in the eastern sector of the developed area, with the intent of confirming that the productive area of the field extends further in this direction. By the middle of the year 2000, the installation of a 27.5 MW plant will complete the development of the area where exploitation is now concentrated. When this unit is in operation, the total installed capacity of the Miravalles field will soon reach 142.5 MW. An additional unit of 19 MW will be installed by 2003 to make use of low-pressure steam to be obtained from a second-stage flash of part of the waste brine.

Of the 45 wells drilled to date, 25 are in use as producers and 11 are used for reinjection of residual water. Another four wells of lower permeability are used to monitor the evolution of reservoir pressure, and three wells drilled at the periphery of the field are available as reserve wells for the reinjection system. Two additional wells are now being drilled.

The main goal of the initial-state modeling was to determine the permeability distribution, recharge and discharge areas, and boundary conditions prevailing in the field before exploitation started. In this context, the most important rock property is permeability. Unlike exploitation modeling, storage-related parameters such as porosity, density and specific heat of the rock are not critical initial-state modeling parameters. Therefore, in initial-state modeling, average values of porosity, density and specific heat of the rock can be used, but more detailed distributions need to be specified for permeability.

Measured subsurface temperatures provide the most reliable calibration criteria for the initial-state modeling; permeabilities in the x, y and z directions are the main variables used in matching measured temperatures. Once a match is obtained by trial and error, it is assumed that the model represents the permeability distribution correctly.

1.2 Description of the Miravalles Initial-State Model

The simulation model for the Miravalles field was oriented in an NS - EW direction. The model includes a total area of 108 km^2 (12 km in the NS direction and 9 km in the EW direction), much larger than the developed area of the field. The large area was required to ensure a reasonable representation of the overall geological framework of the geothermal system and to reduce the effects of the boundary conditions on the simulation model. Figure 1 shows the map of the field and the limit of the model.

In the vertical dimension, the model extends from an elevation of +100 m, mean sea level (msl) to a depth of -1,500 m, msl. The overall thickness of 1,600 m is subdivided into six layers of uneven thickness. The number of gridblocks in each of the layers is not uniform. In the part of the reservoir where the main production zone is located, the number of gridblocks per layer is largest, with each of the three layers containing 365 blocks. The number of gridblocks per layer is reduced to 283 blocks for areas that are above or below the inferred productive zone. The total number of grid blocks in the model is about 2,000.

1.3 Simulation Results

As with most geothermal systems, heat and mass recharge sources and discharge sinks must be present in order to maintain the thermodynamic conditions within the reservoir. After many iterations, it was found that an inflow rate of 226 kg/s was required from the NE recharge source in layer 6, the inflowing water being at a temperature of 255°C. An additional water inflow of 76 kg/s at a temperature of 252°C from the eastern part of layer 6 was required to match the temperature distribution in that part of the reservoir. The discharge from the model is split into several sinks located in layers 1, 2, 3 and 4. The locations of these discharge sinks are dictated by the shape and magnitude of the subsurface temperature contours. Most of the fluid is believed to move toward the southern part of the field, hence the majority of the discharge sinks are located in this area. Figure 2 shows the sites and rates of recharge and discharge as well as the calculated mass flux within layer 2 at the initial-state.

The observed temperature contours, against which the intial-state model was to be calibrated, were constructed based on the initial static temperature surveys of the wells. For example, the observed temperature contours in layer 3 are shown on the lefthand side of Figure 3; temperature data points used in the construction of the contours are also shown on the figure. The majority of these data points are considered fully static and should be reliable. If a data point is not considered fully static, an asterisk is shown next to it to indicate that the temperature was inferred. If two asterisks are placed next to the data point then the temperature was extrapolated and may not be highly reliable. On the right hand side of Figure 3 are shown the calculated temperature distributions in layer 3 of the model, one of the most productive levels of the reservoir. Both the shape and the magnitude of the high temperature lobes are well matched. Similar matches were obtained for the other layers.

To ensure that the thermodynamic parameters of the model do not stray significantly from the observed data, the measured static downhole pressure and temperature profiles of wells were compared to those derived from the model. Such comparison for one of the wells (PGM-10) is illustrated in Figure 4; the measured data are in good agreement with the calculated. It should be noted that while the observed and calculated static pressure profiles have the same gradient (Figure 4), the calculated pressures are about 4 kilograms per square centimeter (ksc) higher than observed at all depths. This difference does not lessen the accuracy of the initial-state model, for the calculated pressure was deliberately kept slightly higher than observed to prevent steam formation within the model in the initial-state, which was close to the boiling point. Suppressing steam formation allows easier calibration of the initial-state model without compromising rigor. Of course, this small, artificial pressure difference was removed before history matching.

2. HISTORICAL DATA MATCHING

The results from the initial-state model of the Miravalles geothermal system show that, after many iterations, a final quantitative model has been derived that satisfactorily matches the initial-state of the reservoir using plausible values of permeability and fluid recharge and discharge rates. We therefore believe that the initial-state model provides a reasonable representation of the overall geothermal system and provides a valid basis for history matching. However, the initial-state model does not provide detailed information on localized reservoir conditions at and near the wells. These parameters are ascertained by matching the historical data from the field.

Of the available historical data, water levels and downhole pressures from observation wells were used to calibrate the model. First, the locations of production and injection zones were specified in the model based primarily on data obtained from flowing downhole surveys. For wells that have no flowing survey data, the production/injection zones were assigned to levels indicated by nearby wells. Then, detailed production and injection data were input into the model, and the observed and calculated pressure trends were matched by trial and error. Production enthalpy data were available but were not particularly useful for matching since the data showed little change during the three years' history. Historical geochemical data trends obtained from the production wells were used to further constrain the model.

The selection of grid blocks to be used for active production wells and observation wells is based on the known completion intervals and locations of the permeable zones in each well. In many cases, the wells were completed in more than one layer of the model and could therefore be responding through multiple layers. To model the separate inflow zones, these wells were assumed to produce from two different layers of the model that correspond to the two major inflow zones.

The comparison between observed and calculated pressures for well PGM-8 is shown in Figure 5. Such closeness of match between the observed and calculated pressure trends was attained for most observation wells.

Consideration was also given to the available historical geochemistry data. These data suggest that a portion of the produced fluid from wells PGM-05 and PGM-10 was derived from the fluid injected into well PGM-22. Similarly, a part of the produced fluid from wells PGM-12, PGM-20, and PGM-21 was of injection origin. The fraction of injection return varies from well to well and ranges from a few percent to 50%. Although these numbers are approximate, this information was incorporated into the model by varying the permeability distribution until an appropriate amount of injection return was obtained at each well.

3. FORECASTING OF RESERVOIR BEHAVIOR

3.1 Introduction

The major question to be answered by the forecast runs was how the reservoir would behave as the generation capacity was increased. A total of three production and injection scenarios were considered:

Scenario 1:
The wells had been supplying 60 MW to Unit 1 since March 1994, and this rate was to be maintained throughout the project life. Originally, Unit 2 was expected to come on-line in May 1998 with an initial generation of 55 MW. Three months later, the capacity of Unit 2 was to be increased to 60 MW, and this rate would continue to the end of the project.

Unit 3 was scheduled to be on-line in May 2000 with a generation capacity of 27.5 MW and the capacity would be maintained to the end of the project. Unit 4 would come on-line in December 2001 and generate 27.5 MW. Injection of fluid at 165°C would be accomplished via wells PGM-22, PGM-24 and new wells in the south and southeastern parts of the field.

Scenario 2:
The production well configuration would remain unchanged. Injection to wells PGM-22 and PGM-24 was to be terminated and then water from these wells diverted to two new south and southeastern wells.

Scenario 3:
This scenario was identical to Scenario 2, except that the injection water temperature was to be 140°C.

3.2 Simulation Results

The field-wide production characteristics plotted on Figures 6 and 7 show that the enthalpy of the production remains constant (Scenario 1) or increases slightly (Scenarios 2 and 3) over the 25 year simulation period. Hence, the injection fluid does not appear to have a major impact on the produced fluid enthalpy over the long term. The combination of the pressure support from wells PGM-22 and PGM-24 and mixing with cooler injection fluid appears to suppress steam formation in the main production zone in Scenario 1.

The enthalpy increases slightly in Scenarios 2 and 3 due to the formation of the two-phase condition in the reservoir. Without the pressure support from the western injectors (PGM-22 and PGM-24), the pressure decline rate in the main production zone is higher compared to the previous case, and a two-phase zone develops. Furthermore, there is no mixing of the cooler injection fluid in this area under these two scenarios. As the Unit 2 wells produce a fluid of slightly lower enthalpy than the present production wells, there is a small decline in enthalpy when Unit 2 starts up. This change is, however, minimal and has little impact on generation. Conversely, wells from Units 3 and 4 are assumed to be located in the northern part of the field near the upflow zone, where the fluid enthalpy is greater than that of the existing wells. Consequently, field-wide fluid enthalpy increases slightly when new units are started in years 6 and 8.

The enthalpy trends shown in Figure 6 for Scenarios 2 and 3 are not identical. The slight difference is due to the density difference between injection fluid at 165°C versus 140°C. Because the 140°C injection water is more dense, it travels downward more easily, causing the minor variation in the field-wide enthalpy trends. It is difficult to predict at this time the onset and the growth of two-phase conditions in the field. Parameters such as non-condensable gas content, local porosity, local permeability, hydraulic connections between injection and production wells, pressure and temperature declines all have major impacts on the phase change phenomenon. Not all of these parameters could be fully accounted for in the model because of the production history being very short and the lack of any enthalpy changes to date. Therefore, the timing of the phase change forecast should be considered approximate.

Pressure decline trends from all three scenarios are depicted in Figure 7. As seen in the figure, the field-wide reservoir pressure declines by about 8 bars for scenario 1 when Unit 2 starts up. For scenarios 2 and 3, the decline is slightly higher because of the absence of the western injectors. After this initial drop, the field-wide pressure continues to decline at a rate of about 0.73 bar/year for scenario 1 and about 1 bar/year for scenarios 2 and 3.

The make-up well requirement is dictated by two main factors, the pressure drop and the evolution of steam saturation in the reservoir. If the field contains single-phase liquid, the calculation of make-up well requirement is relatively easy and accurate. Unfortunately, such is not the case here. Wells in Miravalles are just beginning to produce some free steam. When two-phase conditions develop in a well, the decline rate in well productivity accelerates. At this point, it is difficult to determine exactly when the single phase fluid around a well will become two-phase or to calculate the rate of increase in steam saturation, because there are no clear enthalpy trends yet to calibrate this aspect of the model. With the recent start up of Unit 2, two-phase conditions should become more prevalent and by calibrating the model against the enthalpy trends, the question of make-up well requirement can be answered with confidence.

4. SUMMARY

The results from the simulation runs suggest that the fluid enthalpy remains stable for Scenario 1 and increases very slightly for Scenarios 2 and 3. Injection returns and the encroachment of cool water from the periphery of the field do not appear to pose a problem. In response to additional generation, there is a reservoir pressure drop of about 8 bars upon start-up of Unit 2. The reservoir pressure decline rate for Scenarios 2 and 3 is slightly greater than for Scenario 1 because of the lack of pressure support from injection wells PGM-22 and PGM-24. After the initial pressure drop in May 1998, the reservoir pressure continues to decline at a rate of about 0.73 bar/year in Scenario 1, and 1 bar/year in Scenarios 2 and 3. This pressure drop is the consequence of operating unit 2 at full capacity of 60 MW from the start. If the wells for unit 2 were brought on-line gradually then the initial pressure drop would be reduced.

ACKNOWLEDGEMENTS

The authors wish to express their thanks to ICE (Institudo de Costa Rica Electricidad) for providing the funding for this work, and permission to publish the results of the study. We are also grateful to Dr. Marcelo Lippmann of Lawrence Berkeley National Laboratory for providing a very helpful review of the paper.

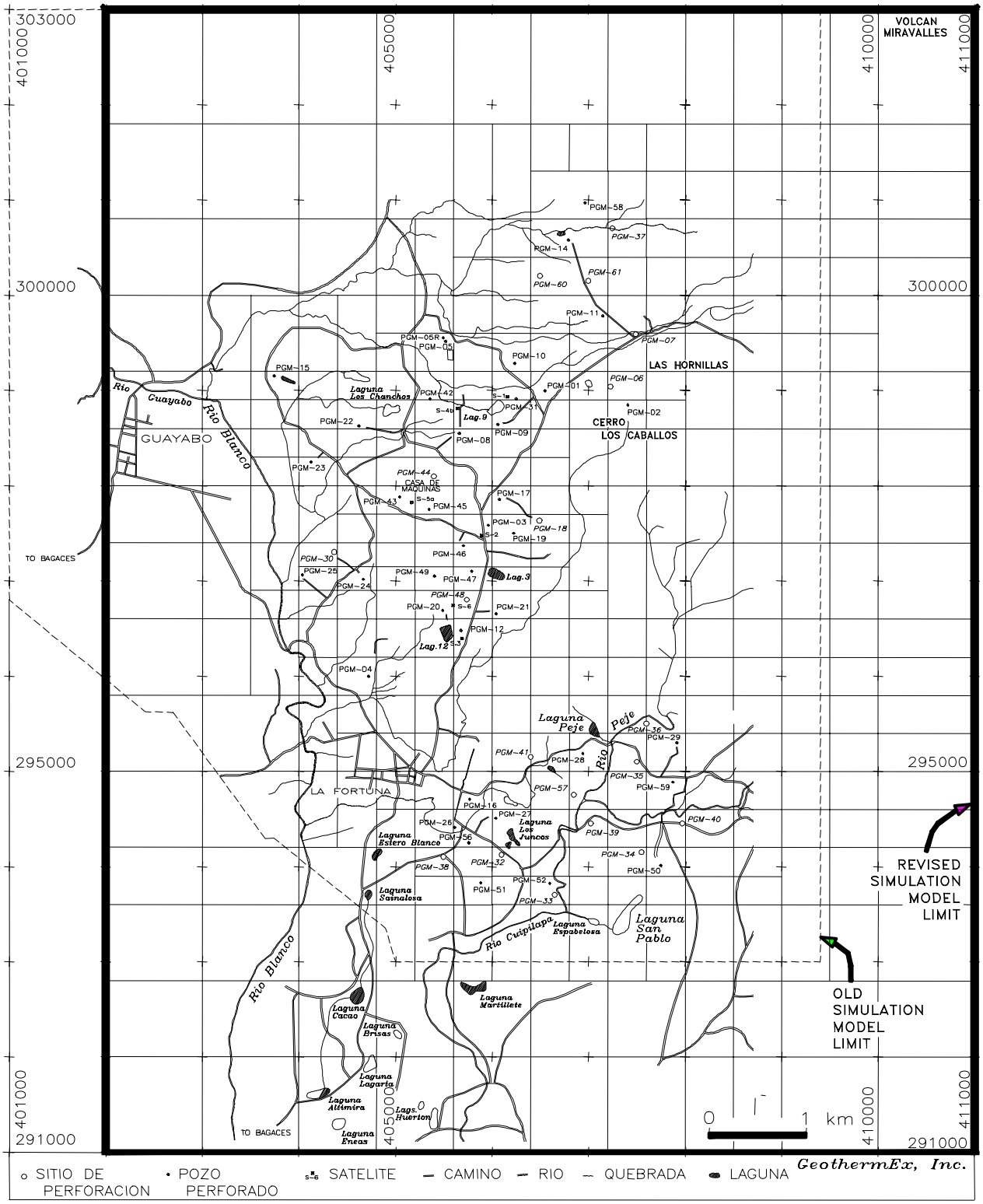

Figure 1. Regional map of Miravalles geothermal files with model limits

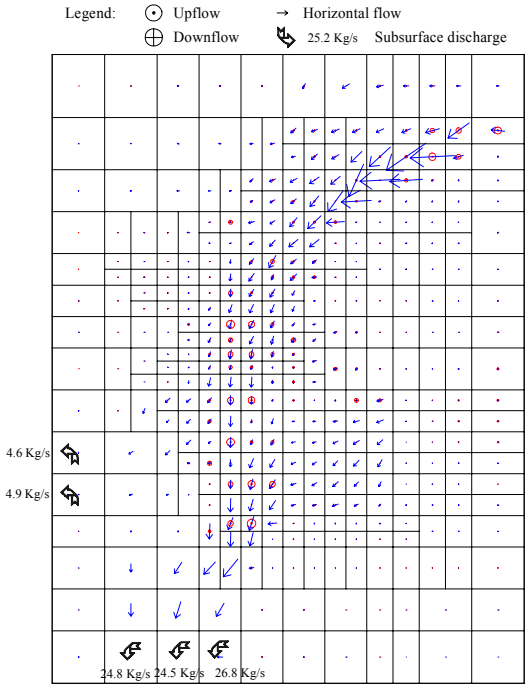

Figure 2. Calculated subsurface massflux, layer 2 @ -300 m, msl

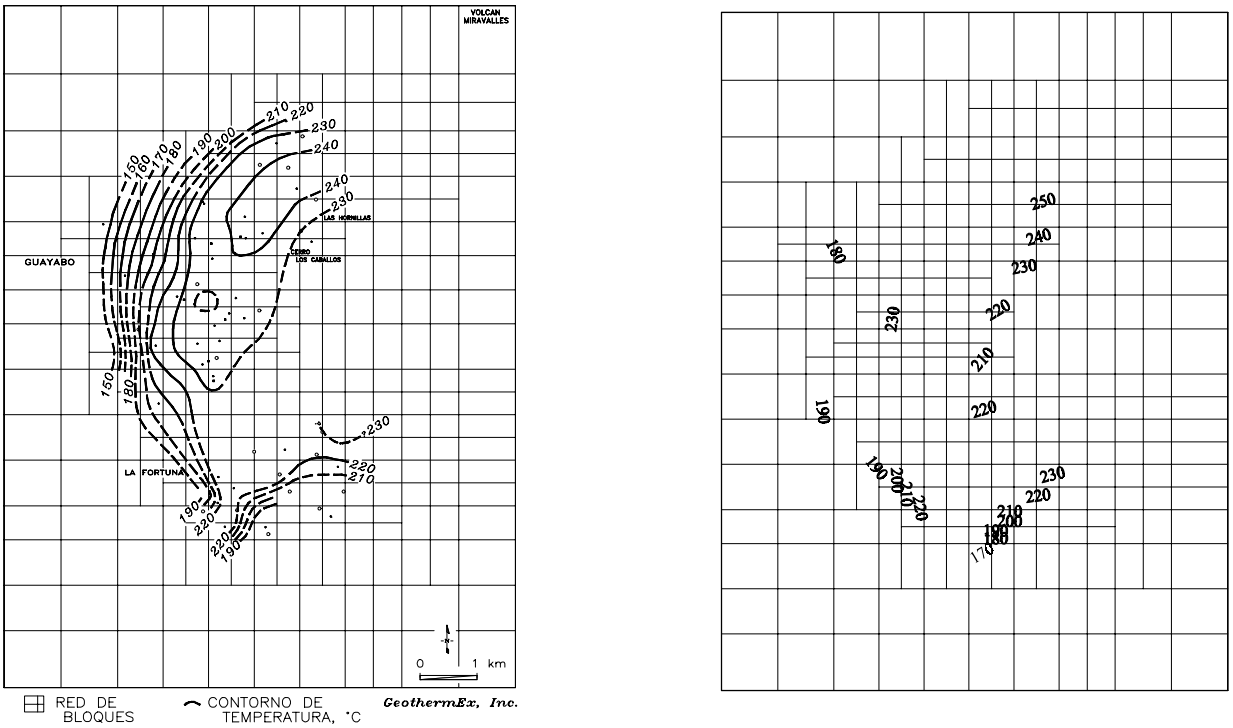

Figure 3. Observed and calculated subsurface temperatures, layer 3 @-500 m, msl

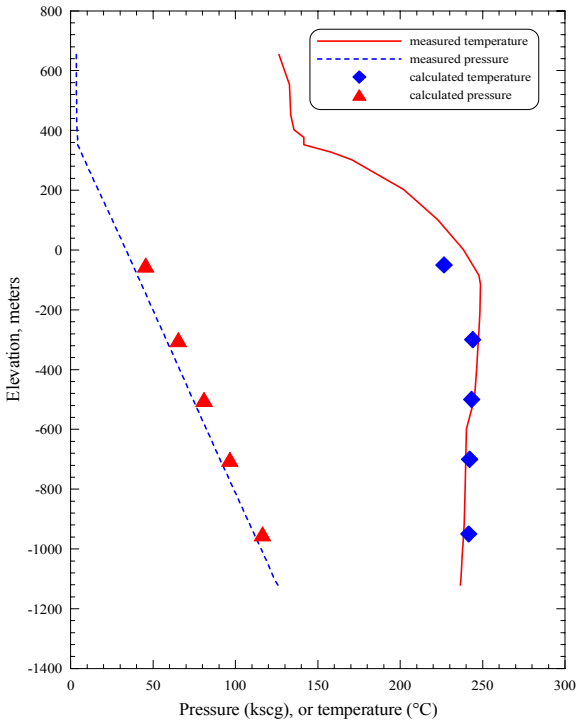

Figure 4. Static pressure and temperature comparison, well PGM10

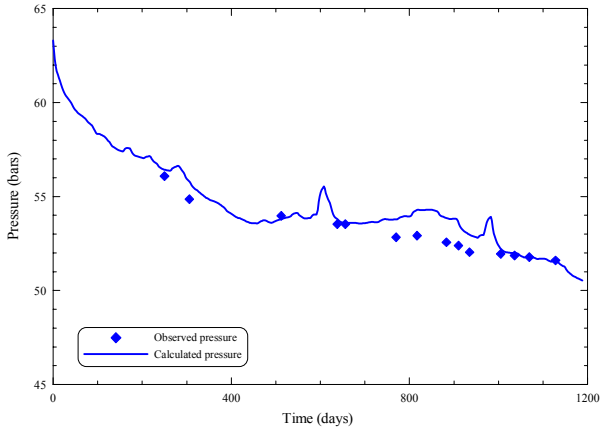

Figure 5. Matching of observed pressure – well PGM08

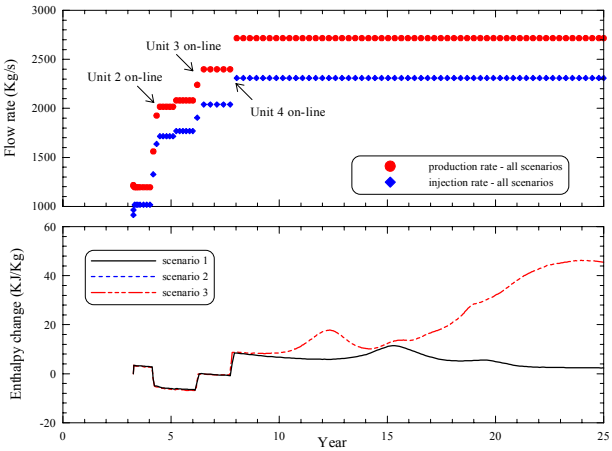

Figure 6. Fieldwide production characteristics – all scenarios

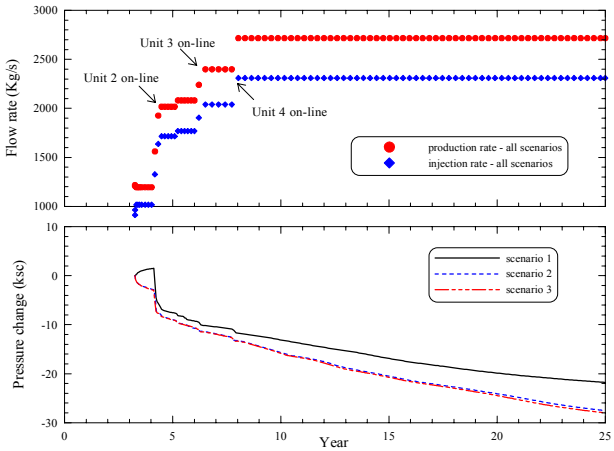

Figure 7. Fieldwide pressure decline rates – all scenarios